

On the stability limits of the hydrogen maser

C. MIRICĂ*, L. GIURGIU

Faculty of Physics, University of Bucharest, PO Box MG 11, București-Măgurele, Romania

A theoretical method for the passive Hydrogen MASER optimization of the operating conditions: interrogation signal level and atomic beam intensity, and of the designing parameters is introduced. The method does not depend on the modulation or the locking technique. The results calculated numerically are plotted, and the relations required determining other quantities of practical interest are provided. A normal full-size MASER and a reduced size one are calculated as example. Theoretical limits of the Hydrogen frequency primary standard stability are deduced (derived). It is demonstrated that the stability limits in passive and active operation coincide and that they ultimately depend by temperature and confinement volume, other influences being possible to be made negligible through electronic enhancement of the quality factor of the reduced size MASER.

(Received March 08, 2010; accepted March 12, 2010)

Keywords: Atomic frequency standards, Hydrogen MASER, Passive operation optimization

1. Introduction

The Hydrogen MASER (Microwave Amplification by Stimulated Emission of Radiation), also known as hydrogen frequency standard, is a specific type of MASER that uses the intrinsic properties of the H atom to serve as a precision frequency reference. Both the proton and electron of a hydrogen atom have spins. The atom has a higher energy if both are spinning in the same direction and a lower energy if they spin in opposite directions. The amount of energy needed to reverse the spin of the electron is equivalent to a photon at the frequency of about 1420 405 752 Hz.

1.1 Electronic model of the MASER cavity

The Hydrogen MASER is a time-frequency standard with an outstanding frequency stability. As physical principle, this MASER uses the atomic Hydrogen resonance at the hyperfine splitting frequency of the Hydrogen atom fundamental level. This transition is used due to the high quality factor of this atomic line (10^9).

The atomic resonance is detected by stimulated emission of radiation in a microwave resonant cavity (of Q_0 quality factor and V_c volume). Within the cavity, the H atoms are confined in a constant phase region (of V_b volume, η' filling factor and T_b storage time) [2].

A magnetically selected atomic beam is collimated in the storage region (of total intensity I_t , having an r proportion of atoms in the useful level $|F=1, m_F=0\rangle$, representing a net intensity $I = rI_t$, the rest being in the level $|F=1, m_F=1\rangle$).

The stored atoms relax through non-radiant processes with the T_1 longitudinal and T_2 transverse relaxation times.

In the passively operated MASER, the resonant cavity is coupled with an input circuit with a coupling factor β_1 , and an output circuit with a coupling factor β_2 . The input

circuit contains a V_1 interrogation voltage generator with a Z_0 matched internal resistance. The output circuit has as load resistance the matched Z_0 input resistance of the amplifier, on which is collected the V_2 voltage. The total coupling factor becomes $\beta = \beta_1 + \beta_2$, that reduces the resonant cavity quality factor to $Q_c = Q_0 / (1 + \beta)$ [2].

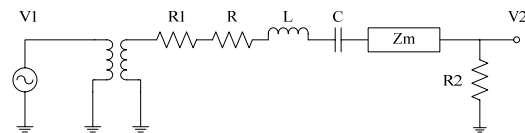


Fig. 1. Equivalent RLC-series electric circuit diagram.

As a matter of principle, the atomic resonance is measured indirectly, through the output microwave voltage of the resonant cavity. The passive mode operation is the general case where there is a interrogation resonant signal injected in the cavity and the perturbation of the output voltage signal is measured through various modulation-demodulation techniques, using the MASER as a very selective microwave quantum amplifier to the purpose of transferring the stability of the atomic resonance to the controlled local oscillator. When this amplifier gets in self-oscillation we have the active mode of operation. The latter mode can occur when the power losses of the cavity and receptor load can be sustained by the power of the coherent stimulated emission of radiation. In such operation, the frequency stability of the atomic resonance line is transferred to a voltage controlled quartz oscillator by phase-locking loop.

Considering that the interrogation voltage has the pulsation $\omega = 2\pi f$, with a $\delta\omega = \omega_0 - \omega$ mistuning correction and that the cavity resonance pulsation is ω_c , with a $\delta\omega_c = \omega_0 - \omega_c$ cavity mistuning correction, than the relation between the generator V_1 and the output V_2 voltages is:

$$V_2 \cdot \left(1 + \beta_1 + \beta_2 + \beta_m + j \cdot \left(\frac{\omega}{\omega_c} - \frac{\omega_c}{\omega} \right) \cdot Q_0 \right) = \sqrt{\beta_1 \cdot \beta_2} \cdot V_1 \quad (1)$$

In a RLC-series model, V_1 the interrogation voltage applies to R_1 internal resistance, R cavity resistance, Z_m active atomic medium impedance, L cavity inductance, C cavity capacity and R_2 load resistance of the detector, on which is collected the output voltage V_2 . All the impedances have the transformed values as measured in the output circuit by the coupling and quality factors.

$$\begin{aligned} R_2 &= Z_0; \quad R = \frac{Z_0}{\beta_2}; \quad R_1 = \frac{\beta_1}{\beta_2} \cdot Z_0; \\ Z_m &= \frac{\beta_m}{\beta_2} \cdot Z_0; \quad L = \frac{Q_0 \cdot Z_0}{2 \cdot \omega_c \cdot \beta_2}; \quad C = \frac{2 \cdot \beta_2}{\omega_c \cdot Q_0 \cdot Z_0} \end{aligned} \quad (2)$$

Using the electronic circuit equivalent (2) the output-input voltages relations (1) can be written as:

$$V_2 \cdot \left[\frac{1 + \frac{R_1}{R} + \frac{R_2}{R} + \frac{Z_m}{R}}{j \cdot \omega \cdot \sqrt{L \cdot C} + \frac{1}{j \cdot \omega \cdot \sqrt{L \cdot C}}} \cdot \frac{1}{R} \cdot \sqrt{\frac{L}{C}} \right] = \frac{\sqrt{R_1 \cdot R_2}}{R} \cdot V_1 \quad (3)$$

The above relation (3) is equivalent to:

$$V_2 = \frac{R_2}{R + R_1 + R_2 + Z_m + \left(j \cdot \omega \cdot L + \frac{1}{j \cdot \omega \cdot C} \right)} \cdot \sqrt{\frac{R_1}{R_2}} \cdot V_1 \quad (4)$$

This expression shows the equivalence with an RLC-series circuit, supplied through a transformer by the interrogation signal voltage.

The impedance Z_m expresses the coupling with the active atomic amplifier, and it has negative values at resonance and becomes null out of resonance, thus the frequency dependency of the output voltage is

$$V_2(\delta\omega) = \frac{\sqrt{\beta_1 \cdot \beta_2}}{1 + \beta + \beta_m(\delta\omega) + j \cdot \frac{\delta\omega_c - \delta\omega}{\omega} \cdot Q_0} \cdot V_1 \quad (5)$$

where β_m is the coupling factor with the atomic medium, and it is a negative quantity due to the signal amplification by stimulated emission.

1.2 Electronic model of the atomic amplifier

For the quantitative description of β_m one should define the quantities related to the effects of spin exchange relaxation and transition saturation. The spin exchange is a non-radiative relaxation that occurs when two atoms collide; hence the process is density and temperature dependent.

Since the threshold intensity I_{th} that has been introduced for the active H MASER has no more physical meaning for the passive MASER [2], another reference and normalized atomic beam intensity are introduced to simplify the definitions:

$$I_{t1} = \frac{2}{T_1} \cdot \frac{1}{\bar{\sigma}_{ex} \cdot \bar{v}_r} \cdot \frac{V_b}{T_b} = \frac{I_{th}}{q}; \quad \tilde{I} = \frac{I_t}{I_{t1}} = q \cdot \frac{I_t}{I_{th}} \quad (6)$$

I_{t1} has the physical meaning of the total atomic beam intensity at which the spin exchange longitudinal relaxation time equals $T_t = \sqrt{(T_1)_0 \cdot (T_2)_0}$ (the geometrical mean of the longitudinal and transverse relaxation times without spin exchange effect); $\bar{\sigma}_{ex}$ is the spin exchange mean cross section; \bar{v}_r is the mean relative velocity between H atoms at the cavity temperature $\Theta_c = 313K$, ($\bar{\sigma}_{ex} \cong 23.3 \cdot 10^{-20} \cdot m^2$, $\bar{v}_r = 3626$ m/s).

In respect to the above mentioned definition, the relaxation time with spin exchange effect can be described as [2]:

$$T_i^{-1} = (T_i)_0^{-1} + i \cdot \tilde{I} \cdot T_i^{-1}, \quad \text{for } i=1 \text{ longitudinal, and } 2 \text{ transversal}$$

Another quantity that should be introduced is the specific quality factor of the Hydrogen MASER, introduced for the unloaded cavity, with a "0" subscript:

$$q_0 = \frac{\bar{\sigma}_{ex} \cdot \bar{v}_r \cdot \hbar}{2 \cdot \mu_0 \cdot \mu_B^2} \cdot \frac{T_b}{T_1} \cdot \frac{1}{\eta' \cdot Q_0 \cdot r} = \frac{q}{1 + \beta} \quad (8)$$

A further simplifying notation is:

$$u = \sqrt{\frac{(T_1)_0}{(T_2)_0}} \in \left[\sqrt{\frac{3}{4}}, 1 \right]; \quad c = 2 \cdot u + u^{-1} \in [2.89, 3] \quad (9)$$

The coupling factor with the atomic active medium becomes:

$$\beta_m = \beta_{m0} \cdot \frac{1 + j \cdot \delta\omega \cdot T_2}{1 + \delta\omega^2 \cdot T_2^2 + S_0} = \frac{\beta_{m0}}{1 + \frac{S_0}{1 + \delta\omega^2 \cdot T_2^2}} \cdot \frac{1 + j \cdot \delta\omega \cdot T_2}{1 + \delta\omega^2 \cdot T_2^2} \quad (10)$$

The unsaturated coupling factor at resonance is defined by

$$\beta_{m0} = - \frac{\tilde{I}}{q_0 \cdot (1 + c \cdot \tilde{I} + 2 \cdot \tilde{I}^2)}; \quad \alpha = - \frac{\beta_{m0}}{1 + \beta} \quad (11)$$

emphasizing the relation with the previously introduced oscillation parameter α [2] that describes the MASER's capacity to enter in oscillation when $\alpha > 1$.

The saturation factor at resonance is:

$$S_0 = \frac{V_{out}^2}{2 \cdot \beta_2 \cdot Z_0 \cdot P_1 \cdot q_0 \cdot (1 + c \cdot \tilde{I} + 2 \cdot \tilde{I}^2)} \quad (12)$$

$$P_1 = \frac{\hbar \cdot \omega_0}{2} \cdot I_{11} \quad (13)$$

The power P_1 has the physical and direct meaning of the potential power brought into the cavity by the magnetically selected atomic beam with the intensity I_{11} , and it's use simplifies all the relations.

The voltage gain produced by the active medium is

$$G = \left(1 + \frac{\beta_m}{1 + \beta}\right)^{-1}; G_0 = \left(1 - \frac{\alpha}{1 + S_0}\right)^{-1} \quad (14)$$

G_0 being the gain at resonance.

2. Method. The optimization theory

In any of the modulation and locking techniques that one might use, the physical quantity whose variation is detected in the passive Hydrogen MASER is the output voltage V_{out} . Considering this reason, the meaningful quantity for the stability evaluation is the dispersion value at resonance:

$$d = \left. \frac{\partial V_{out}}{\partial \omega} \right|_{\delta\omega=0} = V_{out} \Big|_{\delta\omega=0} \cdot T_2 \cdot \frac{\alpha}{1 + S_0 - \alpha \cdot \frac{1 - S_0}{1 + S_0}} \quad (15)$$

Added to the real mistuning voltage, the coupled cavity produces also a noise voltage that has the following value at resonance:

$$V_n = \sqrt{2 \cdot \beta_2 \cdot Z_0} \cdot \sqrt{\frac{4 \cdot k_B \cdot \Theta_c \cdot f}{1 + \beta + \beta_m \Big|_{\delta\omega=0}}} \quad (16)$$

where f is the Fourier frequency band of the filtered noise. It should be mentioned that this is only the thermal white frequency noise of the loaded cavity and it does not contain any other noise source (e.g. inter-modulation noise induced by the modulation technique [3], electronic components flicker noise etc.) that have to be evaluated separately. The white frequency noise approximation is valid for medium time intervals. As for the white frequency noise produced by the phase locking loop, it is to be considered through the amplifier's noise figure that can be measured without any special problem. This approach will be used bellow.

The stability of the VCXO locking, in the assumption that the control loop operates without error, is:

$$\sigma_y(f) = \frac{|\Delta\omega|}{\omega_0} = \frac{V_n(f)}{\omega_0 \cdot \left. \frac{\partial V_{out}}{\partial \omega} \right|_{\delta\omega=0}} \quad (17)$$

due to the presence of the noise voltage V_n that induces a false error signal equal to $\omega_0 d$ in the control loop, shifting

the frequency by $\Delta\omega$. In the time domain, for white noise, the Fourier frequency f transforms to $(2\tau)^{-1}$, τ being the integration time in a stability measurement.

The stability's expression becomes:

$$\sigma_y(\tau) = \frac{1}{\omega_0 \cdot T_1} \cdot \sqrt{\frac{2 \cdot k_B \cdot \Theta_c}{P_1}} \cdot \frac{u + 2 \cdot \bar{I}}{\sqrt{q_0 \cdot (1 + c \cdot \bar{I} + 2 \cdot \bar{I}^2)}} \cdot X(\alpha, S_0) \cdot \tau^{-\frac{1}{2}} \quad (18)$$

where the quantity $X(\alpha, S_0)$ is the dimensionless function:

$$X(\alpha, S_0) = \frac{1 + S_0 - \alpha \cdot \frac{1 - S_0}{1 + S_0}}{\alpha \cdot \sqrt{S_0 \cdot \left(1 - \frac{\alpha}{1 + S_0}\right)}} \quad (19)$$

This result is similar to the expression for the power spectral density of the fractional amplitude fluctuations [2], since it accounts for the envelope detection and amplitude integration of the mistuning voltage.

This quantity is the stability indicator of the interrogation signal level, through the saturation effect, when all the other parameters are kept constant. The first level of optimization is to minimize the X value by finding the optimum saturation for a given oscillation parameter α .

2.1 Saturation level optimization

The study of X , as a function of S_0 having parameter α shows the minimum of this quantity. This minimum is given in two domains of α values, by two roots of the equation $\partial X / \partial S_0 = 0$, providing the optimum relation between S_0 and α :

$$-S_0^4 + (3\alpha - 2)S_0^3 + (3\alpha^2 - 5\alpha + 2)S_0 + (\alpha - 1)^2 = 0$$

$$S_0(\alpha) = \begin{cases} \sqrt{1 - \alpha}; & \text{if } \alpha \leq \frac{8}{9} \\ \frac{3}{2} \cdot \alpha - 1 + \frac{1}{2} \cdot \sqrt{9 \cdot \alpha^2 - 8 \cdot \alpha}; & \text{if } \alpha > \frac{8}{9} \end{cases} \quad (20)$$

By setting the saturation factor according to (20) the number of variables is reduced by one, as in:

$$X(\alpha) = X[\alpha, S_0(\alpha)] \quad (\text{Fig. 2}) \quad (21)$$

leaving the stability to depend on the atomic beam intensity and the MASER quality factor q .

For an already existent MASER, with ionic pumps that do not support atomic beam intensity as high as the optimum level, and with fixed couplings, the optimization stops at this first level.

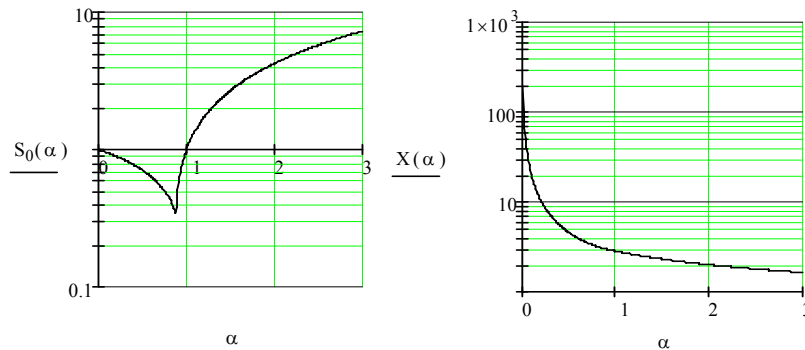


Fig. 2. Optimal saturation S_0 and stability indicator X vs. α .

The optimum saturation factor is to be determined through (20). The output resonance voltage results from (12), and the carrier voltage amplitude V_g of the interrogation signal generator is to be calculated by (5).

2.2 Atomic beam intensity optimization

Since the oscillation parameter α is a function of the beam intensity and of the quality factor:

$$\alpha(q, \tilde{I}) = \frac{\tilde{I}}{q \cdot (1 + c \cdot \tilde{I} + 2 \cdot \tilde{I}^2)} \quad (22)$$

and a parameter of the X stability indicator, the following stability indicator is defined:

$$Y(q, u, \tilde{I}) = \frac{u + 2 \cdot \tilde{I}}{\sqrt{q \cdot (1 + c \cdot \tilde{I} + 2 \cdot \tilde{I}^2)}} \cdot X[\alpha(q, \tilde{I})] \quad (23)$$

to account for the atomic beam intensity influence on the MASER stability.

The second level of optimization is realized by varying the beam intensity to obtain the minimum value of Y, keeping q and u as parameters independent on the operating conditions. This minimum is numerically calculated in the equation:

$$\frac{\partial Y(q, u, \tilde{I})}{\partial \tilde{I}} = 0 \quad (24)$$

The calculated dependence of the normalized beam intensity \tilde{I} and the indicator Y, for $c=3$ (i.e. $(T_1)_0=(T_2)_0$), are plotted in Fig. 3 and, respectively, Fig. 4. For lower values of c, the calculated values of the normalized beam intensity and of the indicator Y are reduced by up to 15%.

The optimum normalized intensity takes values nearby 0.5, with a threshold at $q=3/16=0.188$, when $\alpha=8/9$, where the (15) solution has its first derivative discontinuity. As a comment, it is worth to mention that this result is smaller than [2] that predicts a optimum of 0.845.

The same threshold appears for the stability indicator Y, but, for $q>0.188$, the dependence becomes nearly linear, as predicted in [2].

With the second level of optimization one should determine the optimum normalized beam intensity from Fig. 3 and proceed with the first level of optimization, as described above.

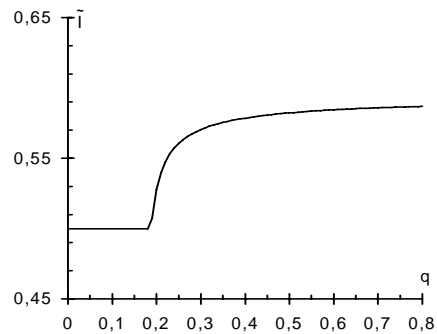


Fig. 3. Optimum normalized intensity for $q<0.8$ and $c=3$.

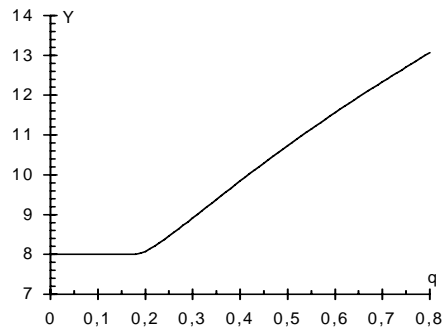


Fig. 4. Optimum stability indicator Y for $q<0.8$ and $c=3$.

For an already existing MASER whose coupling factors cannot be modified, the optimization stops at this level, restricted to the operation parameters: interrogation signal level and atomic beam intensity [5].

The intrinsic stability of the MASER can be determined at this optimization level because the external noise is not introduced yet.

2.3 Resonant cavity coupling factor optimization

In order to determine the optimum coupling factors, the external noise should be considered. The MASER stability, including the external noise, is defined by the following relation:

$$\sigma'_y = \sqrt{F} \cdot \sigma_y \quad (25)$$

using the total input and output noise figure F of the locking loop.

Assuming that β_1 is negligibly small compared to β_2 [2], and considering the equivalent noise temperature (reflected in the output circuit of the cavity) of the amplification chain Θ_a , the noise figure, at resonance, is:

$$F \cong 1 + \frac{1 + \beta + \beta_m}{\beta} \cdot \frac{\Theta_a}{\Theta_c} = 1 + \frac{1 + \beta}{\beta} \cdot \frac{1}{G_0} \cdot \frac{\Theta_a}{\Theta_c} \quad (26)$$

It is easy to observe that low coupling factors increase the noise figure while high coupling factors increase q factor and the Y value. Also, the variation of q implies changes of the optimum value of the gain G_0 . There is an optimum coupling between these two extreme situations, where a third stability indicator named Z

$$Z(q_0, \frac{\Theta_a}{\Theta_c}, \beta) = \sqrt{F} \cdot Y [q_0 \cdot (1 + \beta)] \quad (27)$$

takes the minimum value possible. This optimum total coupling factor is plotted in Fig. 5:

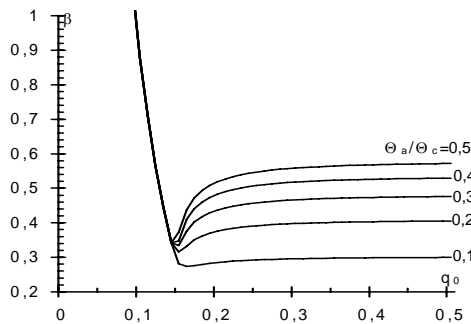


Fig. 5. Optimum coupling factor β for $q_0 < 0.5$, $c = 3$, and ratio $\Theta_a/\Theta_c = 0.1, 0.2, \dots, 0.5$.

For $q_0 < 0.15$, the optimum β is:

$$\beta = \frac{0.188}{q_0} - 1 \quad (28)$$

in order to obtain the threshold value $q = 0.188$ mentioned in sect. 2.5, and this optimum value does not depend on Θ_a .

For $q_0 > 0.15$, the optimum β is numerically calculated from the equation:

$$\frac{\partial Z \left(q_0, \frac{\Theta_a}{\Theta_c}, \beta \right)}{\partial \beta} = 0 \quad (29)$$

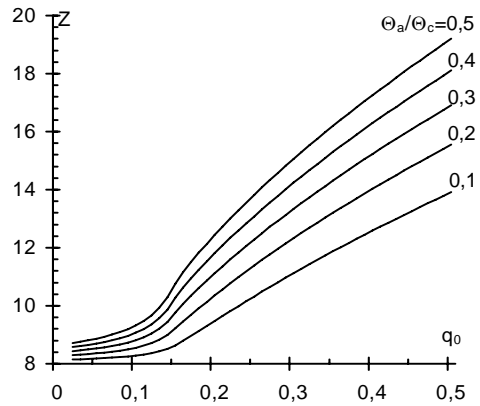


Fig. 6. Calculated optimum stability indicator Z for MASER with quality factors $q_0 < 0.5$, $c = 3$, and ratio $\Theta_a/\Theta_c = 0.1, 0.2, \dots, 0.5$.

Despite that the optimum β has a first derivative discontinuity, the stability indicator Z does not present this discontinuity and tends to Y for Θ_a tending to zero.

This third level of optimization is usable to MASER where the coupling factors can be modified to optimally match them with the control loop noise.

With the coupling factor determined through this last optimization level of the designing parameter β , the previous levels are applicable.

Also, the stability of the MASER can be predicted.

An experimental iterative method to set the optimal values of the operating conditions involves stability measurements and is very difficult.

The other values for resonance gain and for the normalized atomic beam intensity are plotted below, against the unloaded specific MASER quality factor q_0 .

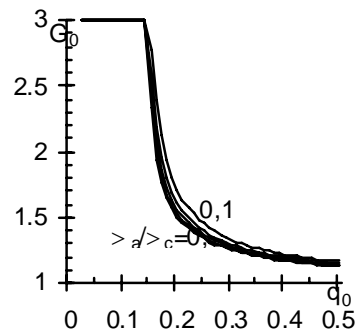


Fig. 7. Calculated optimum resonance gain for MASER with quality factors $q_0 < 0.5$, $c = 3$, and ratio $\Theta_a/\Theta_c = 0.1, 0.2, \dots, 0.5$.

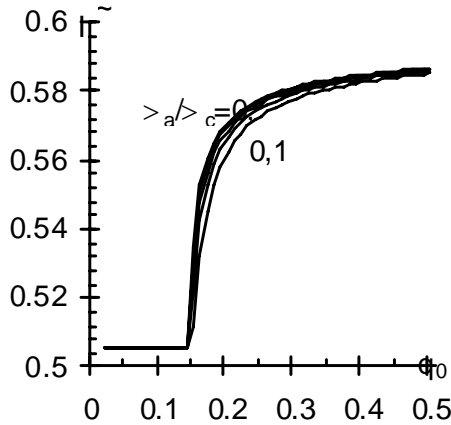


Fig. 8. Calculated optimum normalized intensity for MASER with quality factors $q_0 < 0.5$, $c=3$, and ratio $\Theta_a/\Theta_c = 0.1, 0.2 \dots 0.5$.

3. Results. Example calculations

Table 1. Calculus examples.

Parameter	Full-Size MASER with Saturation Optimization	Full-Size MASER Saturation and Intensity Optimization	Reduced-Size MASER Fully Optimized
Q_0	60.000	60.000	6.000
$V_b [10^{-3} \text{m}^3]$	2,35	2,35	1,15
$T_1 [s]$	0,4	0,4	0,2
q_0	0,0435	0,0435	0,5
Q	0,087	0,087	0,72
$I_{fl} [10^{13}/s]$	2,67	2,67	5,23
\tilde{I}	0,122	0,5	0,59
$P_1 [10^{-11} \text{W}]$	1,26	1,26	2,46
α	1,004	1,916	0,118
S_0	0,911	0,954	0,921
Y	10,1	8,0	17,0
$\sigma_y [10^{-13} \tau^{1/2}]$	0,74	0,59	1,8
Θ_a/Θ_c	75/313	75/313	75/313
β	1	1	0,44
$\sigma'_y [10^{-13} \tau^{1/2}]$	0,82	0,59	2,0

Considering in (9) that $u=1$, $c=3$, for all the practical purposes of $q_0 > 0.15$, the following parameters have the optimal values:

$$\tilde{I} \cong 0,5; \alpha \cong \frac{1}{6q}; \beta_{m0} \cong -\frac{1}{6q_0}; S_0 \cong \sqrt{1-1/6q}; P \cong 3 \cdot q \cdot P_1 \cdot S_0 \quad (30)$$

where P is the total power in the resonant cavity, including the dissipation losses and the output power.

As a result of the above calculations, enhancing the quality factor through feed-back amplification to get

As an exemplification of the above optimization theory, the algorithm was applied to normal and reduced size types of MASER cavities, taken from Tab. 1 of [4].

The first two examples are for a normal size cavity MASER. For all the examples $(T_1)_0 = (T_2)_0$ and $\Theta_a = 75 \text{ K}$ were supposed.

In the first example, the atomic beam intensity was left unchanged and only the saturation factor was optimized.

In the second example the atomic beam intensity was optimized, with a notable improvement of the predicted stability.

In the third example, was considered a reduced size cavity MASER. A full optimization of the coupling factor, beam intensity and saturation was calculated.

$q_0 < 0.15$ provides less penalty in the overall stability through the influence of the amplification noise.

The optimal relative stability of the frequency is:

$$\sigma'_y(\tau) \cdot \sqrt{\tau} \cong \frac{8 \cdot 20}{\omega_0 \cdot T_1} \cdot \sqrt{\frac{2 \cdot k_B \cdot \Theta_c}{P}} \quad (31)$$

$$\sigma'_y(\tau) \cdot \sqrt{\tau} = \frac{Z}{\omega_0} \cdot \sqrt{\frac{2k_B \cdot \Theta_c}{\hbar \cdot \omega_0} \cdot \frac{\bar{\sigma}_{ex} \cdot \bar{v}_t \cdot T_b}{V_b} \cdot \frac{1}{T_1}} \cdot \frac{\Theta_c^{3/4}}{V_b^{1/2}} \quad (32)$$

Ultimately, the stability limit of the hydrogen MASER is related to the temperature and the confining volume. All the other influences can be reduced to negligible in worsening the stability.

As a particular case, when $q_0 < 0,15$ the active operation mode is described by the relations $S_0 = \alpha - 1$ when $V_1 = 0$. From the same method results the same minimal values for the intrinsic stability indicator $Y=8$ as it has been obtained for an optimally operated passive mode. From this mere fact, we have proposed these results as theoretical stability limits.

4. Conclusions

The stability of the output error signal was used as performance criterion for the optimization problem. For the definition of the stability was used the power spectral density of the fractional thermal amplitude fluctuations, because it is the quantity that affects the envelope detection and amplitude integration of the mistuning voltage.

A three level optimization algorithm was developed:

1. the saturation factor optimization: for the MASER were the atomic beam intensity and the coupling factors are given; this level provides the optimum interrogation generator voltage and the corresponding output voltage;

2. the atomic beam intensity optimization: for the MASER were the coupling factors are given; this level is to be followed by the first one;

3. the total coupling factor optimization: for the MASER were the couplings are to be designed, or could be changed; this level takes account on the equivalent noise temperature of the noise of the entire amplification, detection and feed-back loop reflected in the output circuit of the cavity; this level is to be followed by the second one.

The calculated optimal stability according to the above described method applied for comparison to MASER cavities parameters exemplified by [4] have proved to be better than the results of the quoted reference.

All the other practically interesting quantities, such as the voltages, could be easily calculated with the provided relations, in any particular case of specific proportion between β_1 and β_2 .

As a demonstrated conclusion, the only theoretical way to improve the stability is to increase the confinement volume and to decrease the cavity temperature.

Both ways of improving the stability have been experimentally tested by others [1-4]. An increased confining volume reduces the uncertainty introduced by the wall-shift, while cryogenic temperatures increase the so called "wall-shift" due to the hydrogen atoms adsorption to the confinement surface.

Basically with any $q_0 < 0,15$ it can be achieved the operational and design physical limit of stability according to the above described method.

Acknowledgments

The authors would like to express their gratitude to late Prof. Octav C. Gheorghiu, a true mentor who patiently formed generations of specialists with the Atomic Clocks Team in INLPR. We would also like to thank Prof. Tiberiu Tudor for the supportive and fruitful discussions.

References

- [1] G. Busca, IEEE Proc. 33th Ann. Symp. on Freq. Contr., 563, 1979.
- [2] C. Audoin, J. Vanier, The Quantum Physics of Atomic Frequency Standards Adam Hilger, Bristol, 1988.
- [3] C. Audoin, V. Candelier, N. Dimarcq, Conf. on Precision Electromagn. Measurements, 1990.
- [4] C. Audoin, J. Viennet, P. J. Lesage, Physique **42**(C8), 159 (1981).
- [5] C. Mirică, L. C. Giurgiu, O. C. Gheorghiu, Proc. 11-th European Frequency Forum, NEUCHATEL, 4-6 March 1997, 610, 1997.

*Corresponding author: claudiu.mirica@incite.ro